

SUPPLEMENTARY INFORMATION

Supplementary figures

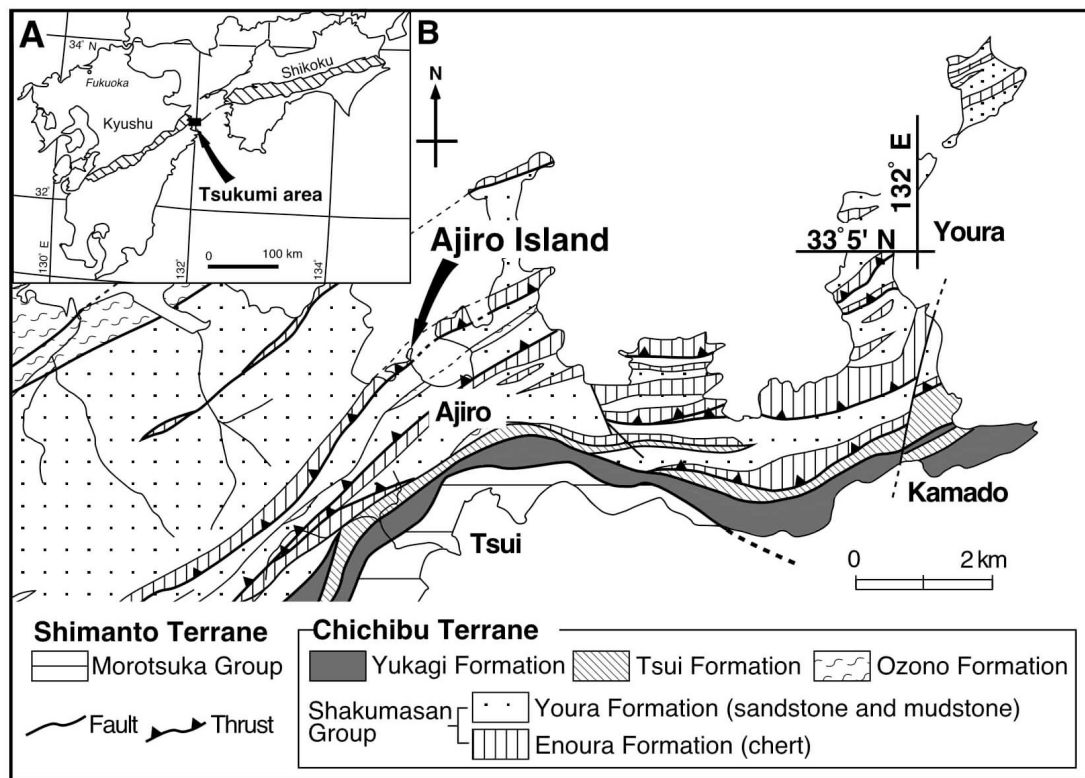


Figure DR1. A: Map showing the approximate distribution of the Chichibu Terrane in southwest Japan and the location of the study area (modified after Nishi, 1994). B: Geologic map showing the location of the studied section on Ajiro Island (33°4'12"N/131°55'11"E). The stratigraphic top and bottom of the Shakumasan Group are truncated by thrust faults. The tectonic slices are repeated due to thrust faulting during subduction and accretion within the accretionary wedge (Matsuoka, 1992).



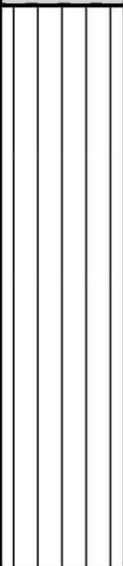
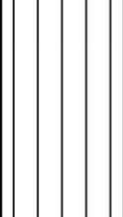
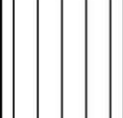

		Lithology	Radiolarian zone	Age			
Shakumasan Group	Youra Formation		Mudstone and Sandstone	JR5 [Tc]	Callovian	Middle	Jurassic
	Enoura Formation		Siliceous mudstone	JR4 [Tp]	Bathonian		
				JR3 [Lj]	Bajocian		
			JR2 [Te]	Aalenian	175.6Ma		
			JR1 [Ps]	Toarcian	Early		
				Pliensbachian			
				Sinemurian			
				Hettangian	199.6		
				Rhaetian			
					Norian	Late	
					Carnian		
					Ladinian		228.7
				Anisian	Middle	245.9	
		Olenekian		Early			

Figure DR2. Time–stratigraphic summary of the Shakumasan Group in the Tsukumi area, western Kyushu, Japan, modified after Nishi (1994). Radiolarian chert of the Shakumasan Group is considered to record the sedimentary history of an oceanic plate prior to accretion at the trench (Matsuoka, 1992; Nishi, 1994). Vertical bar labeled *AJR* indicates the approximate age range of the studied section on Ajiro Island. Triassic and Jurassic radiolarian zones are from Sugiyama (1997) and Matsuoka (1995), respectively. Radiometric ages are after Ogg et al. (2008).

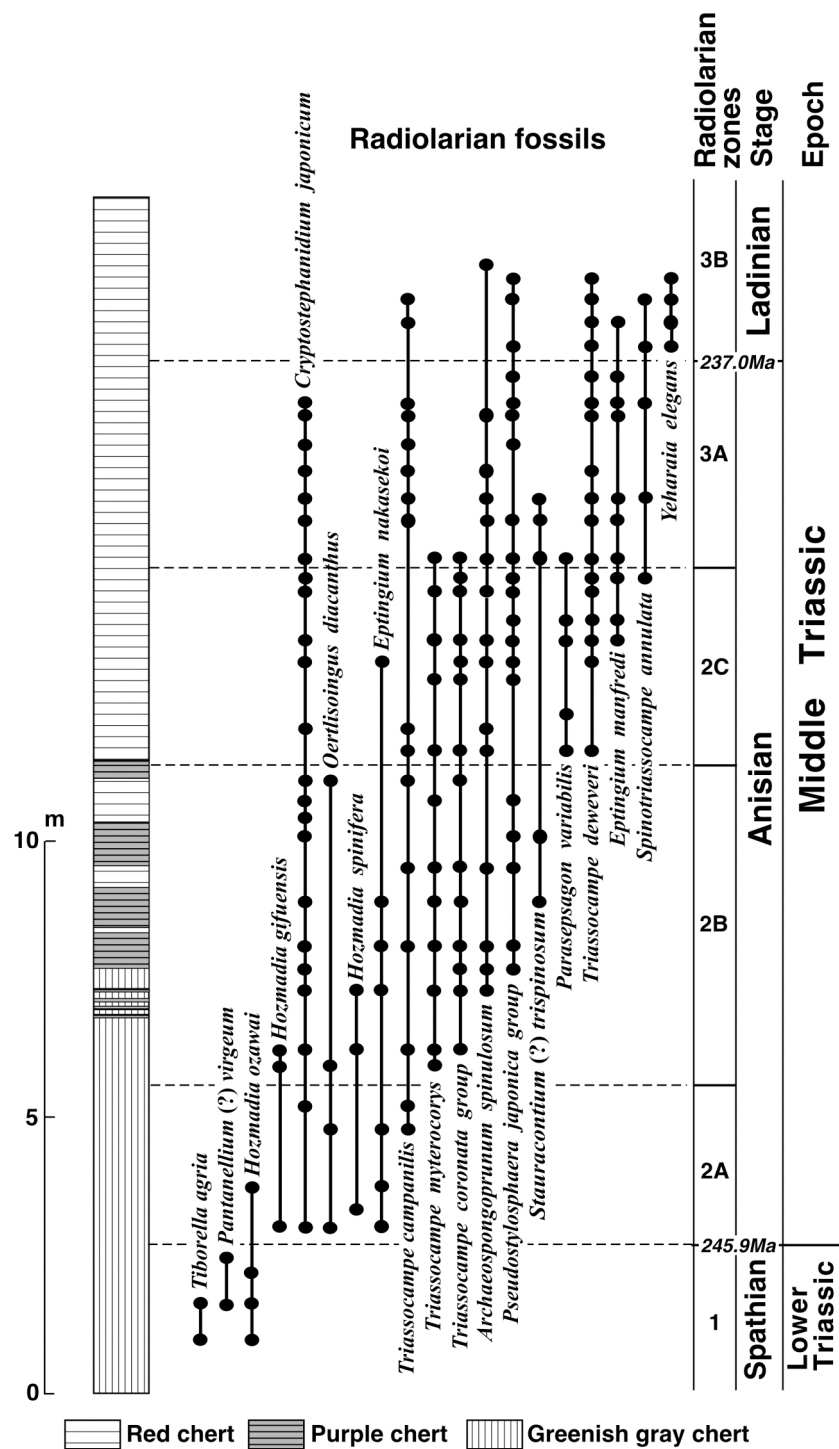


Figure DR3. Lithologic column and stratigraphic distribution of selected radiolarian species in Lower to Middle Triassic chert. Triassic radiolarian zones are from Sugiyama (1997). Radiometric age data are after Ogg et al. (2008).

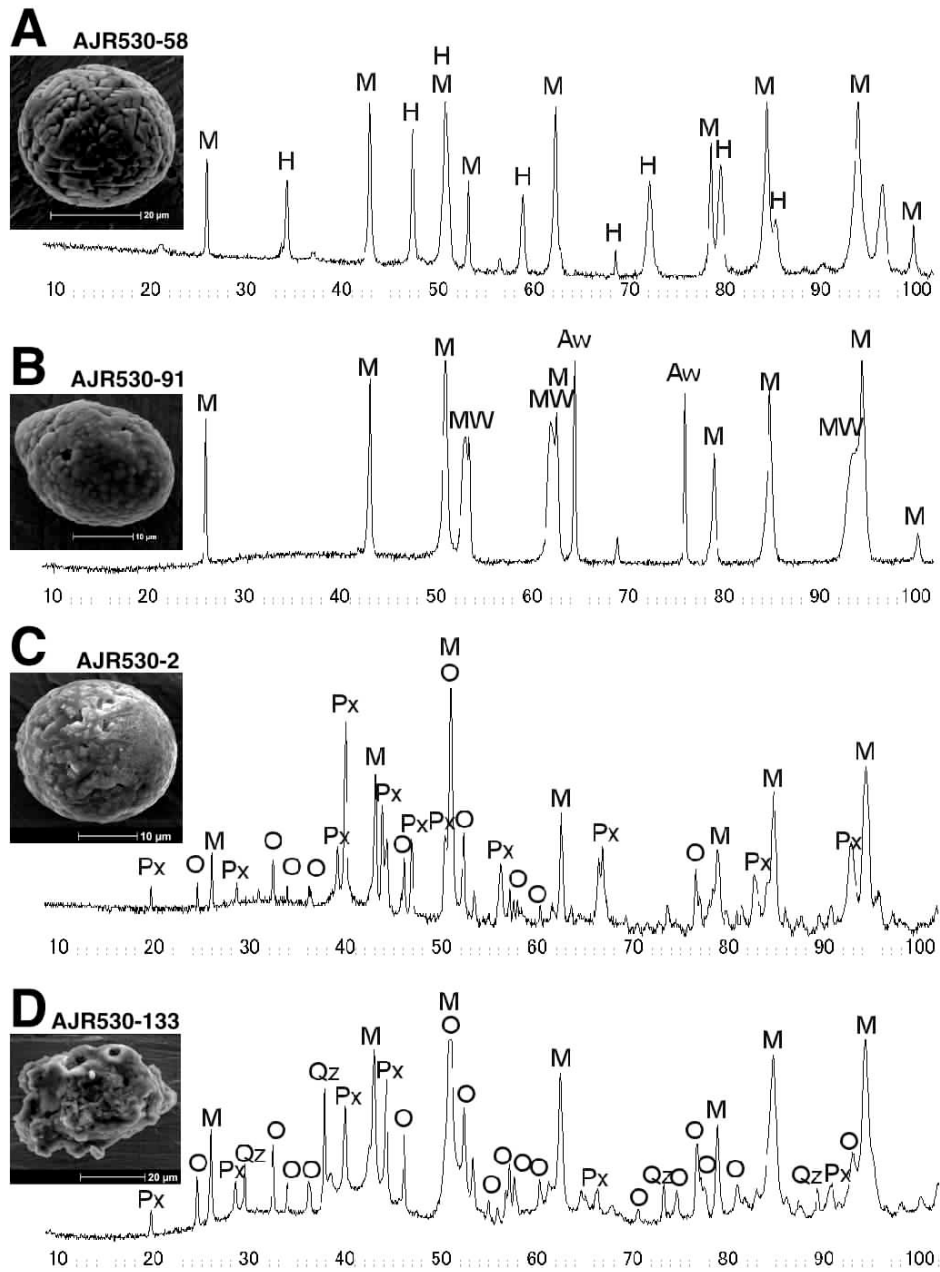


Figure DR4. X-ray diffraction patterns for diffraction angles (2θ) from 10° to 100° and secondary electron micrographs of I-type (A, B) and S-type (C) spherules and unmelted micrometeorite (D). Abbreviations: M = magnetite or maghemite; MW = magnesiowüstite; H = hematite; Aw = awaruite; O = olivine; Px = low-Ca pyroxene; Qz = quartz. The quartz peaks for the unmelted micrometeorite are derived from chert fragments on its surface.

Supplementary table

Table DR1. Sedimentation rates of the Anisian shale in the Middle Triassic chert succession.

Sedimentation rate ratio	Sedimentation rate of shale	Time interval	Total thickness of shale	Total thickness of chert
K	a_1 (mm kyr ⁻¹)	T (kyr)	A (mm)	B (mm)
10	0.55	8900	3705	11998
100	0.43	8900	3705	11998

Note: To estimate the average sedimentation rate of the Anisian shale, we measure the thickness of 625 shale beds and 625 chert beds for the Anisian (Table DR1). The sedimentation rates for shale and chert, a_1 and a_2 , is calculated by the following equations (Sugiyama, 1994), under the assumption that the sedimentation rates were constant within cherts and shale, respectively,

$$T = A/a_1 + B/a_2, \quad (1)$$

$$A = \sum_{i=1}^n A_i, \quad (2)$$

$$B = \sum_{i=1}^n B_i, \quad (3)$$

where n is the total number of beds counted, T is the time interval for the Anisian, and A , and B are the total thickness of the Anisian shale and chert, respectively. Here the sedimentation rates for chert and shale is given by

$$a_2 = Ka_1, \quad (4)$$

where constant K corresponds to the ratio of the sedimentation rate of shale to that of chert. Constant K value of 10 to a maximum value of 100, because the shale bed has a much slower accumulation rate than the chert bed, based on the 10-100 times higher abundance of magnetic microspherules of probable extraterrestrial origin in shale than in chert (Hori et al., 1993). Finally, the average sedimentation rate of the Anisian shale, a_1 , is calculate by

$$a_1 = A/T + B/KT. \quad (5)$$

Table DR2. Bulk composition of the Anisian micrometeorites.

Type	530-133 Unmelted Micrometeorite	530-2 S-type spherule	530-31 S-type spherule	583-34 G-type spherule	396-3 I-type spherule	560-1 I-type spherule
Analysis point		6	5	5	6	5
SiO ₂	36.69	31.39	39.13	18.55	0.10	0.80
TiO ₂	bd	0.02	0.10	0.07	0.02	0.10
Al ₂ O ₃	1.68	1.64	2.09	4.17	0.03	0.41
FeO*	25.17	36.24	28.95	71.74	78.04	85.69
MnO	0.23	0.27	0.49	0.12	0.09	0.06
MgO	22.50	19.38	21.84	0.26	0.08	0.10
CaO	1.39	0.21	0.46	0.32	bd	0.01
Na ₂ O	0.34	0.02	0.20	0.65	0.04	0.08
K ₂ O	0.11	0.04	0.24	0.12	bd	0.12
Cr ₂ O ₃	0.39	0.71	0.25	bd	bd	0.24
NiO	3.87	1.84	2.41	0.02	9.57	1.26
P ₂ O ₅	0.07	0.04	0.05	0.13	0.06	0.09
SO ₃	0.19	bd	bd	0.18	0.04	0.02
Total	92.64	91.81	96.21	96.34	88.13	88.97

FeO*: Total iron as FeO. bd: below detection.

Supplementary references

- Hori, S.R., Cho, C., and Umeda, H., 1993, Origin of cyclicity in Triassic-Jurassic radiolarian bedded cherts of the Mino accretionary complex from Japan: *Island Arc*, v. 3, p. 170-180.
- Matsuoka, A., 1992, Jurassic-Early Cretaceous tectonic evolution of the Southern Chichibu Terrane, Southwest Japan: *Palaeogeography, Palaeoclimatology, Palaeoecology*, v. 96, p. 71-88.
- Matsuoka, A., 1995, Jurassic and Lower Cretaceous radiolarian zonation in Japan and in the western Pacific: *Island Arc*, v. 4, p. 140-153.
- Nishi, T., 1994, Geology and tectonics of the Sambosan Terrane in eastern Kyushu, Southwest Japan -Stratigraphy, sedimentological features and depositional setting of the Shakumasan Group: *Journal of Geological Society of Japan*, v. 100, p. 199-215.
- Ogg, J.G., Ogg, G., and Gradstein, F.M., 2008, *The concise geologic time scale*: Cambridge, Cambridge University Press, 177 p.
- Sugiyama, K., 1997, Triassic and Lower Jurassic radiolarian biostratigraphy in the siliceous claystone and bedded chert units of the southeastern Mino Terrane, Central Japan: *Bulletin of the Mizunami Fossil Museum*, v. 24, p. 79-193.
- Sugiyama, K., Kamioka, K., and Ozawa, T., 1994, Depositional cyclicity and its origin in Triassic bedded chert: *Chikyu Monthly Extra*, v. 10, p. 33-40.